

Strongly anisotropic vortices in dipolar quantum droplets

Guilong Li¹, Zibin Zhao¹, Xunda Jiang¹, Zhaopin Chen², Bin Liu^{1,*}, Boris A. Malomed^{3,4}, and Yongyao Li^{1,5†}

¹*School of Physics and Optoelectronic Engineering, Foshan University, Foshan 528225, China*

²*Physics Department and Solid-State Institute, Technion, Haifa 32000, Israel*

³*Department of Physical Electronics, School of Electrical Engineering, Faculty of Engineering, Tel Aviv University, Tel Aviv 69978, Israel*

⁴*Instituto de Alta Investigación, Universidad de Tarapacá, Casilla 7D, Arica, Chile*

⁵*Guangdong-Hong Kong-Macao Joint Laboratory for Intelligent Micro-Nano Optoelectronic Technology, Foshan University, Foshan 528225, China*

We construct strongly anisotropic quantum droplets with embedded vorticity in the 3D space, with mutually perpendicular vortex axis and polarization of atomic magnetic moments. Stability of these anisotropic vortex quantum droplets (AVQDs) is verified by means of systematic simulations. Their stability area is identified in the parametric plane of the total atom number and scattering length of the contact interactions. We also construct vortex-antivortex-vortex bound states and find their stability region in the parameter space. The application of a torque perpendicular to the vorticity axis gives rise to robust intrinsic oscillations or rotation of the AVQDs. The effect of three-body losses on the AVQD stability is considered too. The results show that the AVQDs can retain the topological structure (vorticity) for a sufficiently long time if the scattering length exceeds a critical value.

Quantum droplets (QDs), representing a novel form of quantum matter, have drawn much interest in recent years [1–13]. These are droplets of an ultra-dilute superfluid maintained by the balance between the mean-field (MF) and beyond-MF effects [14, 15], the latter one being the Lee-Huang-Yang (LHY) correction [16, 17] to the MF nonlinearity induced by quantum fluctuations. QDs have been experimentally observed in dipolar Bose-Einstein condensates (BECs) [18, 19], as well as in binary BECs of nonmagnetic atoms, with quasi-2D [20, 21] and 3D [22–24]. Prior to that, experimental realization of self-trapped BECs in free space solely through MF effect was impossible due to the critical or supercritical collapse instability in the 2D and 3D settings, respectively [25–28] (nevertheless, weakly unstable quasi-2D *Townes solitons* were experimentally created in a binary BEC [29, 30]). QDs in nonmagnetic condensates appear in the isotropic form, whereas their shapes are anisotropic in dipolar BECs [31, 32]. Actually, stable anisotropic quasi-2D fundamental (zero-vorticity) solitons, with the in-plane dipole polarization, can be created in the magnetic BEC in the absence of the LHY correction [33].

The remarkable properties of QDs have been driving extensive work on this topic, such as Monte-Carlo simulations [34–36], collective excitations [37–39], supersolids, [40–45], and Borromean droplets [46], etc. A particularly interesting direction of the studies is embedding vorticity into the self-bound droplets. It is well known that the creation of self-localized vortices in the multi-dimensional space is a challenging issue. The azimuthal instability, which is induced by the underlying attractive nonlinearity, tends to split the 2D vortex ring or 3D

torus (“donut”) into fragments [47–51]. This instability develops faster than the collapse driven by the cubic self-attraction. In QDs, the splitting instability may be arrested by the competition between the MF attraction and LHY self-repulsion, similar to the stabilizing effect of the cubic-quintic nonlinearity in optics models [48–50]. Stable vortex QDs with the winding numbers (topological charge) up to 5 and 2 (at least) were predicted in 2D [52] and 3D geometries [53], respectively. A novel species of semi-discrete vortex QDs was predicted in arrays of one-dimensional traps [54]. These results indicate that the equilibrium state of the LHY-stabilized superfluid provide a versatile platform for the creation of the stable self-bound vortices.

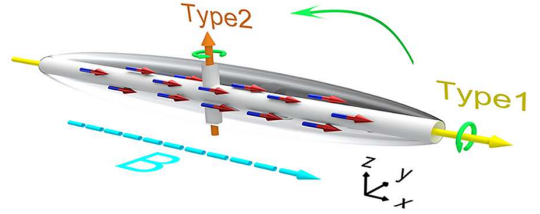


FIG. 1: Possible relations between the vorticity axis and polarization of atomic magnetic dipoles, which is fixed by magnetic field \mathbf{B} along the x axis. Type 1: the vorticity parallel to the polarization (the same as in Ref. [55]). This configuration is always unstable. Type2: the new configuration, which may be stable, with the vorticity oriented perpendicular to the polarization.

The above-mentioned findings were produced for the binary BECs of nonmagnetic atoms. For the dipolar QDs, isotropic vortex modes have been reported, with the vortex axis parallel to the polarization of atomic magnetic moments, represented by “Type 1” in Fig. 1. This configuration is rotationally symmetric with respect to the vorticity axis, but it is unstable [55]. The creation of

*Electronic address: binliu@fosu.edu.cn

†Electronic address: yongyaoli@gmail.com

anisotropic vortex QDs in dipolar BECs and their stability is an open problem. This problem is also relevant in studies of other nonlinear systems, as no example of such states (i.e., anisotropic vortex solitons) in free space was reported. Very recently, the prediction of a stable vortex QD in a 2D dipolar BECs system has been made [56]. However, this problem was not previously addressed in the full 3D geometry.

In this Letter, we predict the existence of *stable* 3D strongly anisotropic vortex quantum droplets (3D-AVQDs) in the dipolar BEC with the magnetic dipoles polarized *perpendicular* to the vortex' axis, corresponding to the "Type 2" configuration in Fig. 1. Note that this consideration is not a straightforward extension of its 2D counterpart. Indeed, the above-mentioned stable fundamental (zero-vorticity) 2D anisotropic solitons in dipolar BEC do not admit any extension into stable 3D solitons in the free space [33]. In the present setting, the anisotropy induced by the orthogonality of the spin polarization and vorticity is fundamentally different in 3D in comparison to the 2D geometry. Moreover, flexural instability can readily set in along the axis perpendicular to the plane of the original 2D mode, thus destroying the stability of the original 2D vortices. Therefore, the stability of the 3D AVQDs is a challenging issue.

The respective 3D LHY-amended Gross-Pitaevskii equation (GPE) is written as

$$i\hbar \frac{\partial}{\partial t} \psi = -\frac{\hbar^2}{2m} \nabla^2 \psi + g|\psi|^2 \psi + \kappa \psi \int U_{\text{dd}}(\mathbf{r} - \mathbf{r}') |\psi(\mathbf{r}')|^2 d\mathbf{r}' + \gamma |\psi|^3 \psi + i\frac{\hbar}{2} L_3 |\psi|^4 \psi, \quad (1)$$

where \hbar and m are the Planck's constant and atomic mass, $g = 4\pi\hbar^2 a_s/m$ with a_s being the s -wave scattering length of inter-atomic collisions, is the strength of the contact nonlinearity, which may be tuned by the Feshbach resonance [57, 58]. The coupling coefficient of the dipole-dipole interaction (DDI) is $\kappa = \mu_0 \mu^2 / 4\pi$, where μ_0 and μ are the vacuum permeability and atomic magnetic moment of the atom. The coefficient in front of the LHY term is $\gamma = \left(32ga_s^{3/2}/3\sqrt{\pi}\right) (1 + 3\epsilon_{\text{dd}}^2/2)$ [59–61], where the relative DDI strength $\epsilon_{\text{dd}} \equiv a_{\text{dd}}/a_s$ is determined by the dipole scattering length, $a_{\text{dd}} = \mu_0 \mu^2 m / 12\pi\hbar$ [18]. The DDI potential is $U_{\text{dd}}(\mathbf{r} - \mathbf{r}') = (1 - 3\cos^2 \Theta) / |\mathbf{r} - \mathbf{r}'|^3$ [62, 63], where $\cos^2 \Theta = (x - x')^2 / |\mathbf{r} - \mathbf{r}'|^2$. Coefficient L_3 represents the three-body losses.

Disregarding the losses, the stationary solutions with chemical potential Ω are looked for in the usual form, $\psi(\mathbf{r}, t) = \phi(\mathbf{r})e^{-i\Omega t/\hbar}$, with a stationary wave function $\phi(\mathbf{r})$. Equation (1) conserves the total atom number, $N = \int |\psi(\mathbf{r})|^2 d\mathbf{r}$, total energy, $E = \int d\mathbf{r} \left[\frac{\hbar^2}{2m} |\nabla \psi|^2 + \frac{1}{2} g |\psi|^4 + \frac{1}{2} \kappa |\psi|^2 \int U_{\text{dd}}(\mathbf{r} - \mathbf{r}') |\psi(\mathbf{r}')|^2 d\mathbf{r}' + \frac{2}{5} \gamma |\psi|^5 \right]$, and the vectorial momentum (here we consider quiescent modes, with zero momentum).

3D-AVQD solutions with integer vorticity S can be produced in the numerical form by means of

the imaginary-time-integration method [64–66], initiated with an anisotropic input,

$$\phi^{(0)}(x, y, z) = A \tilde{r}^S \exp\left(-\alpha_1 \tilde{r}^2 - \alpha_2 z^2 + iS\tilde{\theta}\right), \quad (2)$$

where A and $\alpha_{1,2}$ are positive real constants which determine widths of the input, and the deformed polar coordinates in the (x, y) plane are $\{\tilde{r}, \tilde{\theta}\} \equiv \left\{ \sqrt{x^2 + \beta^2 y^2}, \arctan(\beta y/x) \right\}$ with an anisotropy factor $\beta > 1$. In this work, we select parameters of the BEC of dysprosium, ^{164}Dy , which has a significant dipole length, with $a_{\text{dd}} = 131a_0$ (a_0 is the Bohr radius) [18]. The control parameters of the system are N and a_s .

3D-AVQDs with $S = 1$ can be obtained as numerical solutions of Eq. (1). The stability of the 3D-AVQDs was tested by real-time simulations of perturbed evolution. The numerically found stability area for them in the (N, a_s) plane is shown in Fig. 2(a), with a typical example of a stable 3D-AVQD shown in Fig. 2(b). The average atomic density of this state is 140×10^{20} atoms/m³, in agreement with the prediction of the density in Ref [67]. In the simulations, stable 3D-AVQDs, which populate the blue areas in Fig. 2(a), maintain their integrity during a sufficient long time (at least, ~ 100 ms), which is longer than the levitation time (~ 90 ms) in the experiment [18]. On the other hand, the unstable 3D-AVQDs [in gray area in Fig. 2(a)] spontaneously transform into ground-state QDs after a few milliseconds. It is thus observed that 3D-AVQDs exist at $a_s > 12a_0$, and they are stable at $a_s > 27a_0$.

In the 2D geometry, particular *stable* bound-states with a vortex-antivortex-vortex structure were revealed [56]. Remarkably, similar bound-states can be created in the current 3D setting too, by means of input

$$\begin{aligned} \phi^{(0)} = & \sum_{+,-} A_{\pm} \tilde{r}_{\pm} \exp\left(-\alpha_1 \tilde{r}_{\pm}^2 - \alpha_2 z^2 + i\tilde{\theta}_{\pm}\right) \\ & + A\tilde{r} \exp\left(-\alpha_1 \tilde{r}^2 - \alpha_2 z^2 - i\tilde{\theta}\right). \end{aligned} \quad (3)$$

Here, $A_{\pm} > 0$ and $\alpha_{1,2} > 0$ are real constants, $\tilde{r}_{\pm} \equiv \sqrt{(x \pm x_0)^2 + \beta^2 y^2}$, $\tilde{\theta}_{\pm} \equiv \arctan[\beta y/(x \pm x_0)]$, and x_0 is an appropriately chosen separation, cf. Eq. (2). A typical example of such a stable composite QD with average density 200×10^{20} atoms/m³ is displayed in Fig. 2(c). Its stability area in the plane of (N, a_s) is plotted in the orange area embedded in the broader stability region of the regular 3D-AVQDs in Fig. 2(a). It shows that such stable three-pivot vortex bound-states exist in the region of $30 < a_s/a_0 < 45$ and $1800 < N < 6400$.

As mentioned above, the vortex states with the vorticity axis parallel to the polarization of the dipoles [as shown schematically by "Type 1" in Fig. 1] are completely unstable. Because these solutions are axially isotropic symmetry, we mark them as SYM type in Fig. 3. The 3D-AVQD solutions obtained here are anisotropic, therefore they are marked by the ASY label. Figure 3 displays the comparison of the total energy between the

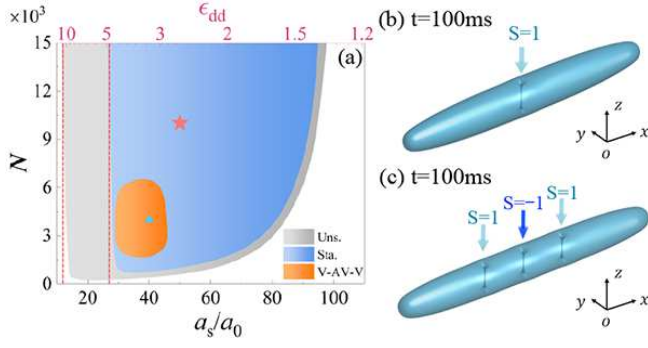


FIG. 2: (a) The areas of stable and unstable 3D-AVQDs, as well as stable vortex-antivortex-vortex bound-states in the plane of (N, a_s) , which populate the blue, gray and orange areas, respectively. The left dashed vertical line, at $a_s = 12a_0$, is the existence boundary for the 3D-AVQDs, and the right vertical line, at $a_s = 27a_0$, is their stability boundary. Red-font numbers, attached to the upper axis, are values of ϵ_{dd} . (b-c) Typical examples of a stable 3D-AVQD and vortex-antivortex-vortex bound-state with $(N, a_s) = (10^4, 50a_0)$ and $(4000, 40a_0)$, corresponding to the red star and blue triangle respectively in panel (a), which survive perturbed evolution during, at least, 100 ms.

isotropic and anisotropic species of the vortex solutions. The energy of fundamental (zero-vorticity) QDs, marked by FUND, is also included, as a reference. Figures 3(a,b) show that the unstable SYM vortex QDs have the highest energy (which is a natural explanation for their instability), while stable ASY vortex states have a lower energy, which is almost identical to that of the fundamental QDs.

For the SYM type of the vortex QDs, the void around the long axis implies the removal of a long tube filled by dipoles chiefly featuring attractive DDIs, i.e., the removal of the negative interaction energy, which causes them to have higher actual energy values, in accordance with Fig. 3(a,b). A typical example of the evolution for this vortex-QD species is displayed in Fig. 3(c1-c3), which demonstrates the instability-induced splitting. These results agree with the instability of the isotropic vortex solitons that was reported in Ref. [55]. On the other hand, the stability of the ASY type is feasible because the corresponding axial void removes a tube filled by dipoles chiefly featuring repulsive DDIs with the positive energy, thus producing lower actual energy values, as corroborated by Fig. 3(a,b). Additional analysis has demonstrated that the application of the imaginary-time-integration method to Eq. (1) does not generate 3D-AVQD solutions with multiple vorticity, $S \geq 2$.

To present systematic results for the 3D-AVQDs, we define their ellipticity \mathcal{A} and normalized angular momentum \bar{L}_z :

$$\mathcal{A} = \frac{D_S}{D_L}, \quad \bar{L}_z = \int \frac{\phi^* \hat{L}_z \phi}{N} dr, \quad (4)$$

where D_S and D_L are, respectively, the short and long axes of the QDs, and $\hat{L}_z = i\hbar(y\partial_x - x\partial_y)$ is the operator

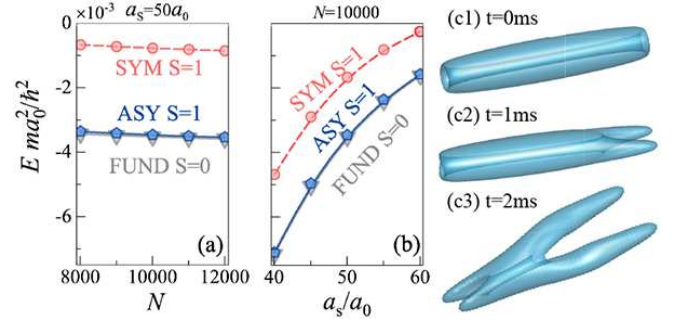


FIG. 3: (a-b) The total energy (E) of the fundamental QDs (the grey curve labeled FUND), 3D-AVQDs (the blue curve labeled ASY), and isotropic vortex QDs (the red curve labeled SYM) versus N (a) and a_s (b). (c1-c3) The unstable evolutions of a SYM vortex QD with $(N, a_s) = (10^4, 50a_0)$ illustrated by its density profiles at $t = 0$ ms, 1 ms, and 2 ms, respectively.

of the z components of the angular momentum. Dependences of the chemical potential, ellipticity, and angular momentum on the number of atoms, for two different values of a_s , are produced in Fig. 4.

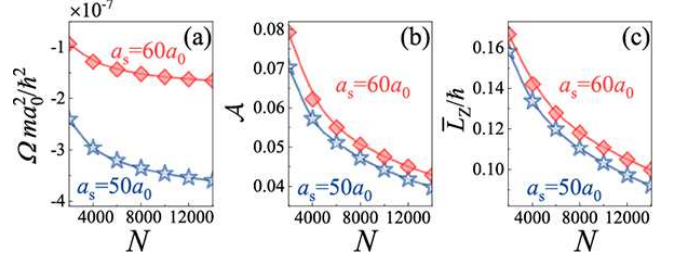


FIG. 4: (a) The chemical potential Ω , (b) ellipticity \mathcal{A} , and (c) angular momentum \bar{L}_z (see Eq. (4)) versus N , for $a_s = 50a_0$ and $60a_0$ (the chains of blue stars and red rhombuses, respectively).

In Fig. 4(a), the chemical potential Ω satisfies the Vakhitov-Kolokolov criterion, $d\Omega/dN < 0$, which is the well-known necessary stability condition for self-trapped modes [26, 68]. A basic feature of QDs is their incompressibility. This implies that the average density of the droplets cannot exceed a maximum value [14], which leads to flat-top QDs' shape. Thus, the volume of the QDs increases linearly with the growth of the number of atoms. Further, due to the strong DDI anisotropy, the increase of the volume is mostly represented by the extension along the x -axis, leading to the decrease of the ellipticity (see Eq. (4)) in Fig. 4(b). As the internal vorticity is mainly concentrated at the center of the droplet, figure 4(c) shows that larger values of norm correspond to longer droplets and lower values of the angular momentum. Moreover, figures 4(b,c) reveal that $\bar{L}_z/\hbar = 2\mathcal{A}$, which coincides with the relation found for strongly anisotropic 2D-AVQDs [56].

The shape of the 3D-AVQDs suggests a possibility to

set it in rotation around an axis perpendicular to the vorticity vector. To this end, a torque was applied around the x -axis, multiplying the established 3D-AVQD by the phase factor $\exp[i(z/z_0)\tanh(y/y_0)]$, i.e., adding an x -component of the angular momentum to the original z -component, cf. Ref. [69]. Here, z_0 and y_0 are length scales, which define the strength of the torque. Simulations reveal oscillations or rotation of the 3D-AVQDs around the x -axis, depending on values of z_0 and y_0 . The weak torque, corresponding to large (z_0 and y_0), induces oscillations, whose period increases with the decrease of z_0 and y_0 . Divergence of the oscillation period implies a transition to the rotation, caused by a sufficiently strong torque (see Movies I and II and in Supplemental Material). The rotation speed increases with the further decrease of y_0 and z_0 , as the torque is made still stronger. Figure 5(a) displays the oscillation and rotation regions in the plane of (z_0^{-1}, y_0) for $(N, a_s) = (10^4, 50a_0)$. The border between these dynamical regimes is fitted by $y_0 = Z_0^2/z_0 + Y_0$, with $Z_0 \approx 0.88 \mu\text{m}$ and $Y_0 \approx 0.06 \mu\text{m}$. This relation is explained by the fact that, for $|y| \lesssim y_0$, the torque's phase, $\approx yz/(y_0z_0)$, is determined solely by the product y_0z_0 . Periods of the oscillations and rotation are displayed, as functions of z_0^{-1} , by insets in the respective regions. A typical example of the stable rotation is presented in Fig. 5(b1-b3). The rotation picture is the same as produced by the stationary solution of Eq. (1) in the rotating reference frame, which includes term $\omega \hat{L}_x \psi$, where $\hat{L}_x = i\hbar(z\partial_y - y\partial_z)$ and ω is the rotation frequency.

We have also explored results of the application of the torque around the y - and z -axes, in terms of Fig. 1. In the former case, the torque drives a complex dynamical regime: the prolate QD features oscillations in the (z, x) plane, simultaneously with irregular rotation around the x axis (not around the y direction), as shown by Movie III in Supplemental Material. Lastly, the application of a weak torque along the z direction initiates oscillations of the prolate vortex soliton in the (x, y) plane (see Movie IV in Supplemental Material), while a stronger torque leads to its splitting, the boundary between the two regimes being $x_0 = Y_0^2/y_0 + X_0$, where $Y_0 \approx 0.67 \mu\text{m}$ and $X_0 \approx -0.5 \mu\text{m}$, in terms of the torque's spatial scales.

Finally, it is imperative to consider the effect of three-body losses, characterized by coefficient $L_3 = 1.25 \times 10^{-41} \text{ m}^6\text{s}^{-1}$ in Eq. (1) [18]. In general, losses usually attenuate instabilities for fundamental (zero-vorticity) states, but this is not applicable to vortex QDs, whose stability is consistently maintained by the equilibrium value of density. We observe that the scattering length a_s significantly affects the loss effect. Notably, for $N = 10^4$, if a_s is smaller than a critical value, $66a_0$, the losses drive rapid degeneration of the initial vortex QD into a fundamental (zero-vorticity) state in the course of < 100 ms (see Movie V in Supplemental Material). The residual state survive much longer, which implies that the QD's topological structure is especially vulnerable to the loss

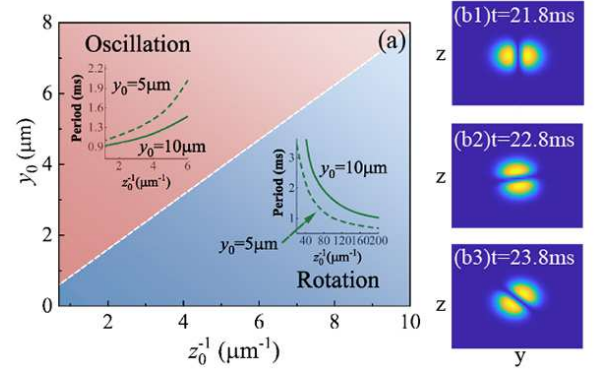


FIG. 5: (a) The oscillation and rotation regions in the plane of the torque's parameters, for $(N, a_s) = (10^4, 50a_0)$. The insets show the oscillation and rotation periods vs. z_0^{-1} for fixed $y_0 = 5$ and $10 \mu\text{m}$ (the dashed and solid lines, respectively). (b1-b3) Plots of the cross-section density in the (y, z) plane illustrating the robust rotation of the 3D-AVQD around the x -axis, with period 5.5 ms, initiated by the torque with $(z_0, y_0) = (0.05, 5) \mu\text{m}$.

effect. However, at $a_s > 66a_0$, the robustness is much improved. For example, as shown in Fig. 6(a-c), the vortex QD with $a_s = 70a_0$ retains its topological charge for more than 400 ms (see Movie VI in Supplemental Material). As shown in Fig. 6(d), in the latter case the total atom number N , effective volume $V = (\int |\psi|^2 d\mathbf{r})^2 / \int |\psi|^4 d\mathbf{r}$, and density $\rho = N/V$ of the QD decrease slowly, demonstrating the losses are not a fatal factor.

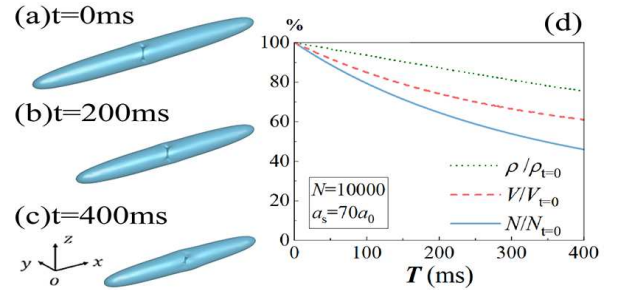


FIG. 6: (a-c) The real-time evolution of the droplet with three-body losses for $N = 10^4$ and $a_s = 70a_0$. (d) The residual ratio of N , V , and ρ versus time.

Conclusion We have predicted stable strongly 3D-AVQDs in dipolar BEC, with mutually perpendicular vorticity vector and polarization of atomic magnetic moments. While isotropic vortex solitons in dipolar BEC are completely unstable, we have identified a vast stability region of 3D-AVQDs in the system's parameter space. The existence of stable composite states with the vortex-antivortex-vortex structure is demonstrated as well, and their stability area is identified. Essential characteristics of the 3D-AVQDs, including the chemical potential, aspect ratio, and angular momentum, are presented as functions of control parameters. Furthermore, we have

demonstrated that the application of the torque perpendicular to the vorticity axis initiates robust intrinsic oscillations or rotation of the 3D-AVQDs. The dependence of the oscillation and rotation periods on parameters of the torque have been found. Persistence of the 3D-AVQDs in the presence of three-body losses was analyzed too, demonstrating that the topological structure (vorticity) is retained by the 3D-AVQD for a sufficiently long time when the scattering length exceeds a critical value.

As an extension of the present analysis, it may be relevant to look for more complex bound states of AVQDs, and to study a two-component version of the model, cf. Refs. [70–72]. Another relevant problem is to add an ingredient (probably, an external potential) that may help to stabilize higher-order vortex droplets, with $S \geq 2$.

Acknowledgments

Authors appreciate a valuable discussion with Prof. Zhenya Yan, Prof. G. E. Astrakharchik, and Xizhou Qin.

This work was supported by NNSFC (China) through Grants No. 12274077, 11874112, 11905032, by the Natural Science Foundation of Guangdong province through Grant No. 2021A1515010214, and 2021A1515111015, the Key Research Projects of General Colleges in Guangdong Province through grant No. 2019KZDXM001, the Research Fund of Guangdong-Hong Kong-Macao Joint Laboratory for Intelligent Micro-Nano Optoelectronic Technology through grant No.2020B1212030010. The work of B.A.M. is supported, in part, by the Israel Science Foundation through grant No. 1695/22.

-
- [1] I. Ferrier-Barbut and T. Pfau, Quantum Liquids Get Thin, *Science* **359**, 274 (2018).
- [2] M. Guo and T. Pfau, A new state of matter of quantum droplets, *Front. Phys.* **16**, 32202 (2021).
- [3] Z. Luo, W. Pang, B. Liu, Y. Li, and B. A. Malomed, A new kind form of liquid matter: Quantum droplets, *Front. Phys.* **16**, 32201 (2021).
- [4] B. A. Malomed, The family of quantum droplets keeps expanding, *Front. Phys.* **16**, 22504 (2021).
- [5] F. Böttcher, J.-N. Schmidt, J. Hertkorn, K. S. H. Ng, S. D. Graham, M. Guo, T. Langen, and T. Pfau, New States of Matter with Fine-Tuned Interactions: Quantum Droplets and Dipolar Supersolids, *Rep. Prog. Phys.* **84**, 012403 (2021).
- [6] L. Chomaz, I. Ferrier-Barbut, F. Ferlaino, B. Laburthe-Tolra, B. L. Lev, and T. Pfau, Dipolar Physics: A Review of Experiments with Magnetic Quantum Gases, *Rep. Prog. Phys.* **86**, 026401 (2023).
- [7] I. Ferrier-Barbut, M. Schmitt, M. Wenzel, H. Kadau, and T. Pfau, Liquid Quantum Droplets of Ultracold Magnetic Atoms, *J. Phys. B: At. Mol. Opt. Phys.* **49**, 214004 (2016).
- [8] G. E. Astrakharchik and B. A. Malomed, Dynamics of one-dimensional quantum droplets, *Phys. Rev. A* **98**, 013631 (2018).
- [9] T. G. Skov, M. G. Skou, N. B. Jørgensen, and J. J. Arlt, Observation of a Lee-Huang-Yang Fluid, *Phys. Rev. Lett.* **126**, 230404 (2021).
- [10] Y.-C. Xiong and L. Yin, Self-Bound Quantum Droplet with Internal Stripe Structure in 1D Spin-Orbit-Coupled Bose Gas, *Chinese Phys. Lett.* **38**, 070301 (2021).
- [11] F. Zhang and L. Yin, Phonon Stability of Quantum Droplets in Dipolar Bose Gases, *Chinese Phys. Lett.* **39**, 060301 (2022).
- [12] Y. Wang, L. Guo, S. Yi, and T. Shi, Theory for Self-Bound States of Dipolar Bose-Einstein Condensates, *Phys. Rev. Research* **2**, 043074 (2020).
- [13] T. A. Yoğurt, U. Tanyeri, A. Keleş and M. Ö. Oktel, Vortex Lattices in Strongly Confined Quantum Droplets, *Phys. Rev. A* **108**, 033315 (2023).
- [14] D. S. Petrov, Quantum Mechanical Stabilization of a Collapsing Bose-Bose Mixture, *Phys. Rev. Lett.* **115**, 155302 (2015).
- [15] D. S. Petrov and G. E. Astrakharchik, Ultradilute Low-Dimensional Liquids, *Phys. Rev. Lett.* **117**, 100401 (2016).
- [16] T. D. Lee, K. Huang, and C. N. Yang, Eigenvalues and eigenfunctions of a Bose system of hard spheres and its low-temperature properties, *Phys. Rev.* **106**, 1135-1145 (1957).
- [17] N. B. Jørgensen, G. M. Bruun, and J. J. Arlt, Dilute Fluid Governed by Quantum Fluctuations, *Phys. Rev. Lett.* **121**, 173403 (2018).
- [18] M. Schmitt, M. Wenzel, F. Böttcher, I. Ferrier-Barbut, and T. Pfau, Self-bound droplets of a dilute magnetic quantum liquid, *Nature* **539**, 259 (2016).
- [19] L. Chomaz, S. Baier, D. Petter, M. J. Mark, F. Wächtler, L. Santos, and F. Ferlaino, Quantum-Fluctuation-Driven Crossover from a Dilute Bose-Einstein Condensate to a Macrodroplet in a Dipolar Quantum Fluid, *Phys. Rev. X* **6**, 041039 (2016).
- [20] C. R. Cabrera, L. Tanzi, J. Sanz, B. Naylor, P. Thomas, P. Cheiney, and L. Tarruell, Quantum Liquid Droplets in a Mixture of Bose-Einstein Condensates, *Science* **359**, 301 (2018).
- [21] P. Cheiney, C. R. Cabrera, J. Sanz, B. Naylor, L. Tanzi, and L. Tarruell, Bright soliton to quantum droplet transition in a mixture of Bose-Einstein condensates, *Phys. Rev. Lett.* **120**, 135301 (2018).
- [22] G. Semeghini, G. Ferioli, L. Masi, C. Mazzinghi, L. Wolswijk, F. Minardi, M. Modugno, G. Modugno, M. Inguscio, and M. Fattori, Self-Bound Quantum Droplets of

- Atomic Mixtures in Free Space, *Phys. Rev. Lett.* **120**, 235301 (2018).
- [23] G. Ferioli, G. Semeghini, L. Masi, G. Giusti, G. Modugno, M. Inguscio, Albert Gallemí, A. Recati, and M. Fattori, Collisions of Self-Bound Quantum Droplets, *Phys. Rev. Lett.* **122**, 090401 (2019).
- [24] C. D’Errico, A. Burchianti, M. Prevedelli, L. Salasnich, F. Ancilotto, M. Modugno, F. Minardi, and C. Fort, Observation of quantum droplets in a heteronuclear bosonic mixture, *Phys. Rev. Res.* **1**, 033155 (2019).
- [25] G. Fibich and G. Papanicolaou, Self-focusing in the perturbed and unperturbed nonlinear Schrödinger equation in critical dimension, *SIAM J. Appl. Math.* **60**, 183 (1999).
- [26] L. Bergé, Wave collapse in physics: principles and applications to light and plasma waves, *Phys. Rep.* **303**, 259 (1998).
- [27] E. A. Kuznetsov and F. Dias, Bifurcations of solitons and their stability, *Phys. Rep.* **507**, 43 (2011).
- [28] C. Pethick and H. Smith, *Bose-Einstein Condensation in Dilute Gases* (Cambridge University Press, Cambridge; New York, 2002).
- [29] C.-A. and C.-L. Hung, Observation of universal quench dynamics and Townes soliton formation from modulational instability in two-dimensional Bose gases, *Phys. Rev. Lett.* **125**, 250401 (2020).
- [30] B. Bakkali-Hassani, C. Maury, Y.-Q. Zhou, E. Le Cerf, R. Saint-Jalm, P. C. M. Castilho, S. Nascimbene, J. Dalibard, and J. Beugnon, Realization of a Townes Soliton in a Two-Component Planar Bose Gas, *Phys. Rev. Lett.* **127**, 023603 (2021).
- [31] D. Baillie, R. M. Wilson, R. N. Bisset, and P. B. Blakie, Self-Bound Dipolar Droplet: A Localized Matter Wave in Free Space, *Phys. Rev. A* **94**, 021602 (2016).
- [32] M. Wenzel, F. Böttcher, J.-N. Schmidt, M. Eisenmann, T. Langen, T. Pfau, and I. Ferrier-Barbut, Anisotropic Superfluid Behavior of a Dipolar Bose-Einstein Condensate, *Phys. Rev. Lett.* **121**, 030401 (2018).
- [33] I. Tikhonenkov, B. A. Malomed, and A. Vardi, Anisotropic solitons in dipolar Bose-Einstein condensates, *Phys. Rev. Lett.* **100**, 090406 (2008).
- [34] M. A. Garcia-March, B. Julia-Diaz, G. E. Astrakharchik, T. Busch, J. Boronat, and A. Polls, Quantum correlations and spatial localization in one-dimensional ultracold bosonic mixtures, *New J. Phys.* **16**, 103004 (2014).
- [35] L. Parisi, G. E. Astrakharchik, and S. Giorgini, Liquid State of One-Dimensional Bose Mixtures: A Quantum Monte Carlo Study, *Phys. Rev. Lett.* **122**, 105302 (2019).
- [36] V. Cikojević, L. V. Markić, M. Pi, M. Barranco, and J. Boronat, Towards a quantum Monte Carlo-based density functional including finite-range effects: Excitation modes of a ^{39}K quantum droplet, *Phys. Rev. A* **102**, 033335 (2020).
- [37] M. Tylutki, G. E. Astrakharchik, B. A. Malomed, D. S. Petrov, Collective excitations of a one-dimensional quantum droplet, *Phys. Rev. A* **101**, 051601(R) (2020).
- [38] H. Hu, and X. Liu, Consistent Theory of Self-Bound Quantum Droplets with Bosonic Pairing, *Phys. Rev. Lett.* **125**, 195302 (2020).
- [39] D. Baillie, R. M. Wilson, and P. B. Blakie, Collective Excitations of Self-Bound Droplets of a Dipolar Quantum Fluid, *Phys. Rev. Lett.* **119**, 255302 (2017).
- [40] Y. Zhang, F. Maucher, and T. Pohl, Supersolidity around a Critical Point in Dipolar Bose-Einstein Condensates, *Phys. Rev. Lett.* **123**, 015301 (2019).
- [41] Y. Zhang, T. Pohl, and F. Maucher, Phases of supersolids in confined dipolar Bose-Einstein condensates, *Phys. Rev. A* **104**, 013310 (2021).
- [42] F. Böttcher, J.-N. Schmidt, M. Wenzel, J. Hertkorn, M. Guo, T. Langen, and T. Pfau, Transient Supersolid Properties in an Array of Dipolar Quantum Droplets, *Phys. Rev. X* **9**, 011051 (2019).
- [43] J. Hertkorn J.-N. Schmidt, M. Guo, F. Böttcher, K. S. H. Ng, S. D. Graham, P. Uerlings, H. P. Büchler, T. Langen, M. Zwierlein, and T. Pfau, Supersolidity in Two-Dimensional Trapped Dipolar Droplet Arrays, *Phys. Rev. Lett.* **127**, 155301 (2021).
- [44] J. Sánchez-Baena, C. Politi, F. Maucher, F. Ferlaino, and T. Pohl, Heating a Dipolar Quantum Fluid into a Solid, *Nat. Commun.* **14**, 1868 (2023).
- [45] D. Scheiermann, L. A. P. Ardila, T. Bland, R. N. Bisset, and L. Santos, Catalyzation of Supersolidity in Binary Dipolar Condensates, *Phys. Rev. A* **107**, L021302 (2023).
- [46] Y. Ma, C. Peng, and X. Cui, Borromean Droplet in Three-Component Ultracold Bose Gases, *Phys. Rev. Lett.* **127**, 043002 (2021).
- [47] B. A. Malomed, *Multidimensional Solitons* (American Institute of Physics: Melville, NY, 2022).
- [48] M. Quiroga-Teixeiro and H. Michinel, Stable azimuthal stationary state in quintic nonlinear optical media, *J. Opt. Soc. Am. B* **14**, 2004-2009 (1997).
- [49] R. L. Pego and H. A. Warchall, Spectrally stable encapsulated vortices for nonlinear Schrödinger equations, *J. Nonlinear Sci.* **12**, 347-394 (2002).
- [50] D. Mihalache, D. Mazilu, L.-C. Crasovan, I. Towers, A. V. Buryak, B. A. Malomed, L. Torner, J. P. Torres, and F. Lederer, Stable spinning optical solitons in three dimensions, *Phys. Rev. Lett.* **88**, 073902 (2002).
- [51] B. A. Malomed, Vortex solitons: Old results and new perspectives, *Physica D* **399**, 108 (2019).
- [52] Y. Li, Z. Chen, Z. Luo, C. Huang, H. Tan, W. Pang, and B. A. Malomed, Two-Dimensional Vortex Quantum Droplets, *Phys. Rev. A* **98**, 063602 (2018).
- [53] Y. V. Kartashov, B. A. Malomed, L. Tarruell, and L. Torner, Three-Dimensional Droplets of Swirling Superfluids, *Phys. Rev. A* **98**, 013612 (2018).
- [54] X. Zhang, X. Xu, Y. Zheng, Z. Chen, B. Liu, C. Huang, B. A. Malomed, and Y. Li, Semidiscrete Quantum Droplets and Vortices, *Phys. Rev. Lett.* **123**, 133901 (2019).
- [55] A. Cidrim, F. E. A. dos Santos, E. A. L. Henn, and T. Macrí, Vortices in self-bound dipolar droplets, *Phys. Rev. A* **98**, 023618 (2018).
- [56] G. Li, X. Jiang, B. Liu, Z. Chen, B. A. Malomed, and Y. Li, Two-Dimensional Anisotropic Vortex Quantum Droplets in Dipolar Bose-Einstein Condensates, *Front. Phys.* **19**, 22202 (2024).
- [57] C. Chin, R. Grimm, P. Julienne, and E. Tiesinga, Feshbach Resonances in Ultracold Gases, *Rev. Mod. Phys.* **82**, 1225 (2010).
- [58] P. Courteille, R. S. Freeland, D. J. Heinzen, F. A. van Abeelen, and B. J. Verhaar, Observation of a Feshbach Resonance in Cold Atom Scattering, *Phys. Rev. Lett.* **81**, 69 (1998).
- [59] R. Schützhold, M. Uhlmann, Y. Xu, and U. R. Fischer, Mean-field Expansion in Bose-Einstein Condensates with Finite-range Interactions, *Int. J. Mod. Phys. B* **20**, 3555 (2006).

- [60] A. R. P. Lima and A. Pelster, Quantum Fluctuations in Dipolar Bose Gases, *Phys. Rev. A* **84**, 041604 (2011).
- [61] F. Wächtler and L. Santos, Quantum Filaments in Dipolar Bose-Einstein Condensates, *Phys. Rev. A* **93**, 061603 (2016).
- [62] T. Lahaye, C. Menotti, L. Santos, M. Lewenstein, and T. Pfau, The Physics of Dipolar Bosonic Quantum Gases, *Rep. Prog. Phys.* **72**, 126401 (2009).
- [63] J. Stuhler, A. Griesmaier, T. Koch, M. Fattori, T. Pfau, S. Giovanazzi, P. Pedri, and L. Santos, Observation of Dipole-Dipole Interaction in a Degenerate Quantum Gas, *Phys. Rev. Lett.* **95**, 150406 (2005).
- [64] L. M. Chiofalo, S. Succi, and P. M. Tosi, Ground state of trapped interacting Bose-Einstein condensates by an explicit imaginary time algorithm, *Phys. Rev. E* **62**, 7438 (2000).
- [65] J. Yang and T. I. Lakoba, Accelerated imaginary-time evolution methods for the computation of solitary waves, *Stud. Appl. Math.* **120**, 265 (2008)
- [66] X. Antoine, W. Bao, and C. Besse, Computational methods for the dynamics of the nonlinear Schrödinger/Gross-Pitaevskii equations, *Comp. Phys. Commun.* **184**, 2621-2633 (2013).
- [67] I. Ferrier-Barbut, H. Kadau, M. Schmitt, M. Wenzel, and T. Pfau, Observation of Quantum Droplets in a Strongly Dipolar Bose Gas, *Phys. Rev. Lett.* **116**, 215301 (2016).
- [68] N. G. Vakhitov and A. A. Kolokolov, Stationary solutions of the wave equation in a medium with nonlinearity saturation, *Radiophys. Quantum Electron.* **16**, 783-789 (1973).
- [69] Y. V. Kartashov, B. A. Malomed, Y. Shnir, and L. Torner, Twisted Toroidal Vortex Solitons in Inhomogeneous Media with Repulsive Nonlinearity, *Phys. Rev. Lett.* **113**, 264101 (2014).
- [70] A. Boudjemâa, Fluctuations and quantum self-bound droplets in a dipolar Bose-Bose mixture, *Phys. Rev. A* **98**, 033612 (2018).
- [71] R. N. Bisset, L. A. P. Ardila, and L. Santos, Quantum Droplets of Dipolar Mixtures, *Phys. Rev. Lett.* **126**, 025301 (2021).
- [72] J. C. Smith, D. Baillie, and P. B. Blakie, Quantum Droplet States of a Binary Magnetic Gas, *Phys. Rev. Lett.* **126**, 025302 (2021).